Synthesis and Characterization of Vanadium(II,III,IV) Complexes of Pyridine-2-thiolate

John G. Reynolds,*,† Shawn C. Sendlinger,‡ Ann M. Murray,† John C. Huffman,‡ and George Christou*,‡

Department of Chemistry and Molecular Structure Center, Indiana University, Bloomington, Indiana 47405-4001, and Lawrence Livermore National Laboratory, University of California, Mail Stop L-365, P. O. Box 808, Livermore, California 94551

Received March 31, 1995[⊗]

The synthesis and characterization are reported of vanadium complexes of pyridine-2-thiolate (pyt^-) with the metal in oxidation states II, III, and IV. The reaction of $VOCl_2(THF)_2$ with 2 equiv of Na(pyt) in THF leads to formation of $[V_2O_2(pyt)_4]$ (**1**). Complex $\mathbf{1}\cdot 2THF\cdot {}^1/_3C_6H_{12}$ crystallizes in hexagonal space group $R\bar{3}$ with the following cell dimensions at −171 °C: $a = b = 30.888(21)$ Å, $c = 8.960(6)$ Å, $Z = 9$, and $V = 7402.8$ Å^3. A total of 1310 unique reflections with $F > 2.33\sigma(F)$ were employed for structure solution and refinement to R (R_w) values of 0.0613 (0.0563). The structure consists of two $VO(pyt)_2$ units joined together by two monoatomic bridges provided by S atoms of two pyt^- groups. The V··V distance is 3.989(2) Å. The reaction of $VCl_3(THF)_3$ with four equivalents of Na(pyt) in THF gives $[VNa(pyt)_4(THF)_2]$ (**2**). Complex **2** crystallizes in triclinic space group $P\bar{1}$ with the following unit cell dimensions at −171 °C: $a = 10.442(2)$ Å, $b = 16.476(4)$ Å, $c = 9.465(2)$Å , $\alpha = 100.73(4)°$, $\beta = 109.20(4)°$, $\gamma = 87.86(3)°$, $Z = 2$, and $V = 1510.3$ Å^3. A total of 3391 unique reflections with $F > 2.33\sigma(F)$ were employed for structure solution and refinement to R (R_w) values of 0.0412 (0.0431). The structure is best described as a heterodinuclear complex with the metals monoatomically bridged by S atoms from three pyt^- groups. The V is seven-coordinate, and the Na is six-coordinate. The V··Na distance is 3.516(1) Å. The reaction of $VCl_2(tmeda)_2$ (tmeda = tetramethylethylenediamine) with 2 equiv of Na(pyt) in THF or CH_2Cl_2 yields $[V(pyt)_2(tmeda)]$ (**3**). Complex **3** crystallizes in orthorhombic space group $B22_12$ with the following cell dimensions at −170 °C: $a = 14.338(5)$ Å, $b = 17.755(7)$ Å, $c = 7.255(2)$ Å, $Z = 4$, and $V = 1846.9$Å^3. A total of 1192 unique reflections with $F > 2.33\sigma(F)$ were employed for structure solution and refinement to R (R_w) values of 0.0220 (0.0261). The complex contains chelating pyt^- and tmeda groups with severely distorted octahedral geometry. Complexes **1**, **2**, and **3** have been characterized by EPR and/or IR spectroscopy. In addition, mass spectral studies are described for **1** and **2**, directed toward identifying fragmentation pathways involving C−S bond cleavage within the pyt^- group; the latter cleavage is detected in the mass spectra of both compounds.

Introduction

In the conversion of crude oils to transportation fuels, many large-scale refining processes utilize heterogeneous catalysts.[1] These catalysts facilitate specialized chemistry, including carbon skeleton cracking and rearrangement, hydrogenation, desulfurization, and denitrification. Suspended and solubilized metal complexes in feedstocks lead to deactivation of such heterogeneous catalysts. The main oil-soluble metal impurities are vanadium and nickel, and crude oils can contain large amounts of soluble vanadyl (VO^{2+}) impurities that are believed to possess two types of ligand environment,[2] the vanadyl petroporphyrins, which have been well-studied and characterized,[3] and the vanadyl non-porphyrins, whose ligand environment is thought to contain S, N, and/or O-donor ligands.[4] The presence of these vanadyl impurities leads to the formation of vanadium sulfides (primarily V_2S_3 and V_3S_4) under the reducing and sulfur-rich hydrotreating conditions.[5−9] These sulfides have deleterious consequences on the activity and lifetime of the supported heterogeneous catalyst (e.g., Mo/Co/S on alumina) employed for crude oil upgrading by causing pore plugging and surface attrition. To model the progressive reduction, sulfiding, and aggregation of crude oil VO^{2+} impurities to vanadium sulfide polymers, we have studied a variety of discrete vanadium−sulfur species in the nuclearity range 1−6 and oxidation state range III−V containing a number of thiolate ligands.[10−17] More recently, we have incorporated into these studies the ligand pyridine-2-thiol (pytH) because (i) it contains functional groups common in crude oils (thiolate-*S* and aromatic-*N*), and (ii) it

† University of California.
‡ Indiana University.
⊗ Abstract published in *Advance ACS Abstracts,* October 1, 1995.

(1) Speight, J. G. *The Chemistry and Technology of Petroleum*; Chemical Industries 3; Marcel Dekker, Inc.: New York, 1980.
(2) Yen, T. F. *The Role of Trace Metals in Petroleum*; Ann Arbor Science: Ann Arbor, MI, 1975; Chapter 1.
(3) Psundararaman, P. *Anal. Chem.* **1986**, *57*, 2204.
(4) Reynolds, J. G.; Gallegos, E. J.; Fish, R. H.; Komlenic, J. J. *Energy Fuels* **1987**, *1*, 36.
(5) Silbernagel, B. G.; Mohan, R. R.; Singhal, G. H. *ACS Symp. Ser.* **1984**, *248*, 91.
(6) Silbernagel, B. G. *J. Catal.* **1979**, *56*, 315.
(7) Asaoka, S.; Nakata, S.; Takeuchi, C. *ACS Symp. Ser.* **1987**, *344*, 275.
(8) Rose-Brussin, M.; Moranta, D. *Appl. Catal.* **1984**, *11*, 85.
(9) Mitchell, P. C. H.; Scott, C. E.; Bonnelle, J.-P.; Grimblot, J. G. *J. Chem. Soc., Faraday Trans. 1* **1985**, *81*, 1047.
(10) Money, J. K.; Huffman, J. C.; Christou, G. *Inorg. Chem.* **1985**, *24*, 3297.
(11) Money, J. K.; Folting, K.; Huffman, J. C.; Collison, D.; Temperly, J.; Mabbs, F. E.; Christou, G. *Inorg. Chem.* **1986**, *25*, 4583.
(12) Money, J. K.; Nicholson, J. R.; Huffman, J. C.; Christou, G. *Inorg. Chem.* **1986**, *25*, 4072.
(13) Money, J. K.; Huffman, J. C.; Christou, G. *J. Am. Chem. Soc.* **1987**, *109*, 2210.
(14) Money, J. K.; Folting, K.; Huffman, J. C.; Christou, G. *Inorg. Chem.* **1987**, *26*, 944.
(15) Money, J. K.; Huffman, J. C.; Christou, G. *Inorg. Chem.* **1988**, *27*, 507.
(16) Christou, G.; Heinrich, D. D.; Money, J. K.; Rambo, J. R.; Huffman, J. C.; Folting, K. *Polyhedron* **1989**, *8*, 1723.
(17) Heinrich, D. D.; Folting, K.; Huffman, J. C.; Reynolds, J. G.; Christou, G. *Inorg. Chem.* **1991**, *30*, 300.

0020-1669/95/1334-5745$09.00/0

has the ability to both chelate and bridge transition metals, potentially allowing access to both mononuclear and oligonuclear products.

The pyt$^-$ ligand has been shown to be capable of binding to transition metals in a number of different ways. Single-crystal X-ray analyses of many complexes have established binding modes **I**−**IV** to be those most commonly observed. Of these,

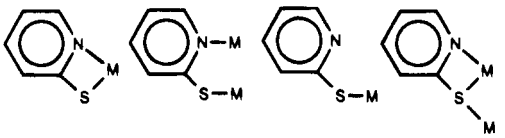

I II III IV

the most common is the bidentate, chelating mode **I**.[18−32a] Several complexes contain η^1:η^1:μ-pyt$^-$ (mode **II**)[33−39] or η^1:η^2:μ-pyt$^-$ (mode **IV**)[40,41] groups, and there are also examples where two modes are to be found in the same complex.[23,26,38,42,43] Some complexes also contain pyt$^-$ groups binding to more than two metals.[38,41−44]

We herein report the results of an investigation directed toward the preparation of vanadium/pyt$^-$ complexes spanning the oxidation state range II−IV. We show that complexes at all three oxidation levels have been successfully obtained and describe the results of subsequent spectroscopic and mass spectral analyses. A preliminary account of this work has appeared.[45]

Experimental Section

All syntheses were carried out under a dinitrogen atmosphere employing standard Schlenk glassware and techniques. Air-sensitive samples for spectroscopic study were prepared and handled in either a dinitrogen glovebag (VWR) or a Vacuum Atmospheres glovebox. All reagents were obtained from Aldrich, unless otherwise indicated. Spectroanalytical grade (Burdick and Jackson) CH_2Cl_2 (0.006% H_2O), hexanes, and THF were dried over CaH_2 (Alfa), $LiAlH_4$, and $LiAlH_4$ followed by Na/benzophenone, respectively. Pyridine-2-thiol (pytH) and *N*,*N*,*N*′,*N*′-tetramethylethylenediamine (tmeda) were used as received; single crystals of pytH were grown from CH_2Cl_2/hexanes. $VOCl_2(THF)_2$[46a] and $VCl_3(THF)_3$[46b] were prepared as described; the former was recrystallized from THF/hexanes. $VCl_2(tmeda)_2$ was prepared from $[V_2Cl_3(THF)_6]_2[Zn_2Cl_6]$[47] by the method of Edema *et al.*[48] Na(pyt) was prepared by the reaction of NaH with pytH in THF, precipitated with hexanes, and recrystallized from THF/hexanes.

$[V_2O_2(pyt)_4]$ (1). A solution of Na(pyt) (1.89 g, 14.2 mmol) in THF (200 mL) was added to a stirred, blue-green solution of $VOCl_2(THF)_2$ (2.00 g, 7.09 mmol) in THF (50 mL). The solution rapidly turned dark brown. After several hours, the solvent was removed *in vacuo* and the residue dissolved in CH_2Cl_2 (100 mL) and filtered. Storage of the filtrate at −10 °C overnight yielded dark brown crystals. These were collected by filtration, washed with hexanes, and dried *in vacuo* to give a brown powder in 40% yield. The product can be recrystallized from CH_2Cl_2/ hexanes or THF/hexanes layerings. The crystallographic sample was obtained by filtering the initial reaction mixture through a fine frit and layering the filtrate with hexanes; the resultant crystals of $1{\cdot}2THF{\cdot}{}^1/_3C_6H_{12}$ lose solvent extremely rapidly when removed from their mother liquor. A vacuum-dried sample analyzed as solvent-free. Anal. Calcd (found) for $C_{20}H_{16}N_4O_2S_4V_2$: C, 41.81 (42.19); H, 2.81 (3.18); N, 9.75 (9.92); S, 22.32 (22.95). Selected IR data, cm^{-1}: 1585 (s), 1552 (m), 1450 (s), 1407 (s), 1269 (m), 1141 (s), 972 (vs), 901 (b).

$[VNa(pyt)_4(THF)_2]$ (2). A solution of Na(pyt) (2.85 g, 21.4 mmol) in THF (200 mL) was added to a stirred, red solution of $VCl_3(THF)_3$ (2.00 g, 5.35 mmol) in THF (100 mL). The solution rapidly turned deep blue-black, and then slowly converted to a deep blood-red over the course of 6 h. The next day, the solution was filtered through a fine frit and the filtrate stored at −10 °C for 3 days. The resultant black crystals were collected by filtration and recrystallized from THF/ hexanes or CH_2Cl_2/hexanes layerings at −10 °C. Yields were typically ~60%. Anal. Calcd (found) for $C_{28}H_{32}N_4O_2S_4NaV$: C, 51.05 (50.93); H, 4.90 (4.82); N, 8.50 (8.32)%. Selected IR data, cm^{-1}: 1577 (s), 1549 (m), 1444 (s), 1416 (s), 1254 (m), 1138 (s), 1055 (m), 902 (b).

(18) (a) Rosenfield, S. G.; Berends, H. P.; Gelmini, L.; Stephen, D. W.; Mascharak, P. K. *Inorg. Chem.* **1987**, *26*, 2792. (b) Rosenfield, S. G.; Swedberg, S. A.; Arora, S. K.; Masarak, P. K. *Inorg. Chem.* **1986**, *25*, 2109.

(19) (a) Block, E.; Ofori-Okai, G.; Kang, H.; Wu, J.; Zubieta, J. *Inorg. Chem.* **1991**, *30*, 4784. (b) Block, E.; Kang, H.; Ofori-Okai, G.; Zubieta, J. *Inorg. Chim. Acta* **1991**, *188*, 61.

(20) (a) Constable, E. C.; Palmer, C. A.; Tocher, D. A. *Inorg. Chim. Acta* **1990**, *176*, 57. (b) Constable, E. C.; Raithby, P. R. *Inorg. Chim. Acta* **1991**, *183*, 21.

(21) Cotton, F. A.; Fanwick, P. E.; Fitch, J. W., III. *Inorg. Chem.* **1978**, *17*, 3254.

(22) Schmidt, W.; Henkel, G.; Krebs, B. *Proc. Int. Conf. Coord. Chem.* **1990**, *28*, 1. This conference abstract includes the structure of (PPh_4)-$[V(pyt)_3]$.

(23) Deeming, A. J.; Hardcastle, K. I.; Meah, M. N.; Bates, P. A.; Dawes, H. M.; Hursthouse, M. B. *J. Chem. Soc., Dalton Trans.* **1988**, 227.

(24) (a) Kita, M.; Yamanari, K.; Shimura, Y. *Bull. Chem. Soc. Jpn.* **1989**, *62*, 3081. (b) Masaki, M.; Matsunami, S.; Ueda, H. *Bull. Chem. Soc. Jpn.* **1978**, *51*, 3298.

(25) (a) Preut, H.; Huber, F.; Hengstmann, K.-H. *Acta Crystallogr., Sect. C* **1988**, *44*, 468. (b) Boualam, M.; Meunier-Piret, J.; Biesemans, M.; Willem, R.; Gielen, M. *Inorg. Chim. Acta* **1992**, *198*, 249.

(26) (a) Deeming, A. J.; Meah, M. N.; Randle, N. P.; Hardcastle, K. I. *J. Chem. Soc., Dalton Trans.* **1989**, 2211. (b) Tiekink, E. R. T.; Lobana, T. S.; Singh, R. *J. Cryst. Spectrosc.* **1991**, *21*, 205.

(27) (a) Mura, P.; Robinson, S. D. *Acta Crystallogr.* **1984**, *C40*, 1798. (b) Mura, P.; Olby, B. G.; Robinson, S. D. *J. Chem. Soc., Dalton Trans.* **1985**, 2101.

(28) Castro, R.; Duran, M.; Garcia-Vazquez, J.; Romero, A.; Sousa, A.; Castineiras, W.; Hiller, W.; Strahle, J. *J. Chem. Soc., Dalton Trans.* **1990**, 531.

(29) Deeming, A.; Karim, M.; Powell, N. I. *J. Chem. Soc., Dalton Trans.* **1990**, 2321.

(30) Nakatsu, Y.; Nakamura, Y.; Matsumoto, K.; Ooi, S. *Inorg. Chim. Acta* **1992**, *196*, 81.

(31) Fletcher, S. R.; Skapski, A. C. *J. Chem. Soc., Dalton Trans.* **1972**, 635.

(32) (a) Henkel, G.; Krebs, B.; Schmidt, W. *Angew. Chem., Int. Ed. Engl.* **1992** *31*, 1366. (b) Tsagkalides, W.; Rodewald, D.; Rehder, D. *J. Chem. Soc., Chem. Commun.* **1995**, 165.

(33) (a) Deeming, A. J.; Meah, M. N.; Dawes, H. M.; Hursthouse, M. B. *J. Organomet. Chem.* **1986**, *299*, C25. (b) Kumar, R.; de Mel, V. S.; Oliver, J. P. *Organometallics* **1989**, *8*, 2488.

(34) Ciriano, M. A.; Perez-Torrente, J. J.; Viguri, F.; Lahoz, F. J.; Oro, L. A.; Tiripicchio, A.; Tiripicchio-Camellini, M. *J. Chem. Soc., Dalton Trans.* **1989**, 25.

(35) Umakoshi, K.; Kinoshita, I.; Fukui-Yasuba, Y.; Matsumoto, K.; Ooi, S.; Nakai, H.; Shiro, M. *J. Chem. Soc., Dalton Trans.* **1989**, 815.

(36) Umakoshi, K.; Kinoshita, I.; Ichimura, A.; Ooi, S. *Inorg. Chem.* **1987**, *26*, 3551.

(37) (a) Deeming, A. J. Meah, M. N.; Bates, P. A.; Hursthouse, M. B. *J. Chem. Soc., Dalton Trans.* **1988**, 2193. (b) Zhang, N.; Wilson, S. R.; Shapley, P. A. *Organometallics* **1988**, *7*, 1126.

(38) Umakoshi, K.; Ichimura, A.; Kinoshita, I.; Ooi, S. *Inorg. Chem.* **1990**, *29*, 4005.

(39) Yamamoto, J. H.; Yoshida, W.; Jensen, C. M. *Inorg. Chem.* **1991**, *30*, 1353.

(40) Hursthouse, M. B.; Khan, O. F. Z.; Mazid, M.; Motevalli, M.; O'Brien, P. *Polyhedron* **1990**, *9*, 541.

(41) (a) Cockerton, B.; Deeming, A. J.; Karim, M.; Hardcastle, K. I. *J. Chem. Soc., Dalton Trans.* **1991**, 431. (b) Deeming, A. J.; Karim, M.; Powell, N. I.; Hardcastle, K. I. *Polyhedron* **1990**, *9*, 623.

(42) Oro, L. A.; Ciriano, M. A.; Viguri, F.; Tiripicchio, A.; Tiripicchio-Camellini, M.; Lahoz, F. J. *Nouv. J. Chim.* **1986**, *10*, 75.

(43) (a) Deeming, A. J.; Meah, M. N.; Bates, P. A.; Hursthouse, M. B. *J. Chem. Soc., Dalton Trans.* **1988**, 235. (b) Kiroshita, T.; Yasuba, Y.; Matsumoto, K.; Ooi, S. *Inorg. Chim. Acta* **1983**, *80*, L13.

(44) Kitagawa, S.; Munakata, M.; Shimono, H.; Matsuyama, S.; Masuda, H. *J. Chem. Soc., Dalton Trans.* **1990**, 2105.

(45) Reynolds, J. G.; Sendlinger, S. C.; Murray, A. M.; Huffman, J. C.; Christou, G. *Angew. Chem., Int. Ed. Engl.* **1992**, *31*, 1253.

(46) (a) Kern, R. J. *J. Inorg. Nucl. Chem.* **1962**, *24*, 1105. (b) Manzer, L. E. *Inorg. Synth.* **1982**, *21*, 135.

(47) Canish, J. A. M.; Cotton, F. A.; Duraj, S. A.; Roth, W. J. *Polyhedron* **1987**, *6*, 1433.

(48) Edema, J. J. H.; Stauthamer, W.; Bolhuis, F.; Gambarotta, S.; Smeets, W. J. J.; Spek, A. L. *Inorg. Chem.* **1990**, *29*, 1302.

Table 1. Crystallographic Data for Complexes **1**·2THF·$^1/_3C_6H_{12}$, **2**, **3**, and pytH

	1·2THF·$^1/_3C_6H_{12}$	**2**	**3**	pytH
formula[a]	$C_{30}H_{36}N_4O_4S_4V_2$	$C_{28}H_{32}N_4O_2S_4NaV$	$C_{16}H_{24}N_4S_2V$	C_5H_5NS
fw	373.38	658.76	387.45	111.16
space group	$R\bar{3}$	$P\bar{1}$	$B22_12$	$P2_1/c$
a, Å	30.888(21)	10.442(2)	14.338(5)	6.044(1)
b, Å	30.888(21)	16.476(4)	17.755(7)	6.273(1)
c, Å	8.960(6)	9.465(2)	7.255(2)	14.146(2)
α, deg	90	100.73(4)	90	90
β, deg	90	109.20(4)	90	101.93
γ, deg	120	87.86(3)	90	90
V, Å^3	7402.84	1510.33	1846.86	524.77
Z	9	2	4	4
T, °C	−171	−171	−171	−157
radiation[b]	0.71069	0.71069	0.71069	0.71069
ρ_{calc}, g/cm^3	1.508	1.449	1.393	1.407
μ, cm^{-1}	8.337	6.290	7.405	4.476
no. of obsd data ($F > 3\sigma(F)$)	1310	3391	1192	631
R (R_w)[c]	6.13 (5.63)	4.12 (4.31)	2.20 (2.61)	2.46 (3.05)

[a] Including solvate molecules. [b] Graphite monochromator. [c] $R = \sum||F_o| - |F_c||/\sum|F_o|$. $R_w = [\sum w(|F_o| - |F_c|)^2/\sum w|F_o|^2]^{1/2}$ where $w = 1/\sigma^2(|F_o|)$.

[V(pyt)$_2$(tmeda)] (3). $VCl_2(tmeda)_2$ (0.500 g, 1.41 mmol) and Na(pyt) (0.380 g, 2.85 mmol) were dissolved with stirring in THF (45 mL) to give a deep purple-red solution. The reaction mixture was stirred overnight and the solvent removed *in vacuo*. The purple residue was dissolved in CH_2Cl_2 (20 mL), filtered to remove NaCl, and the solvent removed *in vacuo* to give a deep purple solid in essentially quantitative yield. Black crystals suitable for crystallography were obtained from a THF solution layered with hexanes (3:4 v/v). Repeated attempts to obtain an elemental analysis were unsuccessful, the results being highly variable even on the same sample, and we assign this to the extreme sensitivity of the complex. Selected IR data, cm^{-1}: 1576 (s), 1549 (m), 1443 (s), 1416 (s), 1254 (m), 1138 (m), 1126 (m), 1053 (m), 901 (b).

X-ray Crystallography. Data were collected using a Picker four-circle diffractometer; details of the diffractometry, low-temperature facilities, and computational procedures employed by the Molecular Structure Center are available elsewhere.[49] Suitable crystals were located, affixed to the end of a glass fiber using silicone grease, and transferred to the goniostat where they were cooled for characterization and data collection. Inert-atmosphere handling techniques were employed. Data collection parameters are summarized in Table 1. The structures were solved using the standard combination of direct methods (MULTAN) and Fourier techniques, and refined by full-matrix least-squares methods. No absorption corrections were performed.

For complex **1**·2THF·$^1/_3C_6H_{12}$, a systematic search of a limited hemisphere of reciprocal space yielded a set of reflections whose Laue symmetry indicated the space group to be either $R3$ or $R\bar{3}$. Choice of the centrosymmetric space group $R\bar{3}$ was confirmed by subsequent successful solution and refinement of the structure. The positions of the V and S atoms were obtained from an initial E-map, and the remainder of the non-hydrogen atoms were found in subsequent iterations of least-squares refinement and difference Fourier map calculations. The structure consists of a $V_2O_2(pyt)_4$ molecule lying on an inversion center, a THF molecule in a general position and displaying disorder of one C atom (C(21)), and a C_6H_{12} molecule lying on a $\bar{3}$ site (occupancy 0.33).

For complex **2**, a systematic search of a limited hemisphere of reciprocal space located a set of diffraction maxima with no symmetry or systematic absences, indicating a triclinic space group. Subsequent structure solution and refinement confirmed the centrosymmetric space group $P\bar{1}$. All non-hydrogen atoms were readily located and refined anisotropically; there was no sign of any disorder problems. Hydrogen atoms were clearly visible in a difference Fourier map phased on the non-hydrogen atoms, and they were allowed to vary in the final refinement cycles with isotropic thermal parameters. A final difference map was featureless, the largest peak being 0.43 e/Å^3.

For complex **3**, a systematic search of a limited hemisphere of reciprocal space located a set of diffraction maxima with systematic absences and symmetry corresponding to the unique orthorhombic space group $B22_12$ (an alternate setting of $C222_1$). Subsequent solution and refinement confirmed this choice. All non-hydrogen atoms were readily located and showed no signs of disorder. They were refined with anisotropic thermal parameters. All hydrogen atoms were visible in a difference Fourier map phased on the non-hydrogen atoms, and they were included in the final least-squares cycles and refined isotropically. The reported structure is the correct absolute structure, on the basis of examination of the final residuals after changing the signs of the anomalous dispersion terms. A final difference Fourier map was featureless, the largest peak being 0.21 e/Å^3.

For pytH (**4**), a systematic search of a limited hemisphere of reciprocal space revealed symmetry and systematic absences consistent with space group $P2_1/c$, which was confirmed by the successful solution of the structure. After the non-hydrogen atoms had been located and partially refined, a difference Fourier map revealed all of the hydrogen positions. In the final cycles of least-squares refinement, the non-hydrogen atoms were refined with anisotropic thermal parameters and the hydrogen atoms were refined with isotropic thermal parameters. The final difference map was essentially featureless, the largest peak being 0.2 e/Å^3.

Other Measurements. IR spectra were recorded as KBr pellets or Nujol mulls on a Mattson Polaris Model 10410 FTIR, a Nicolet 510P FTIR, or a Perkin-Elmer 283 IR spectrometer. Electronic spectra were recorded on CH_2Cl_2 or THF solutions using a Hewlett-Packard Model 8452A diode-array spectrophotometer and Spectrocell R-2010-T quartz anaerobic cells. Mass spectra were recorded on a VG 7070E mass spectrometer in the electron-impact positive ion mode. EPR spectra were recorded on a Bruker ESP 300 spectrometer. Elemental analyses were performed by Galbraith Laboratories.

Results

Syntheses. A number of synthetic procedures have been employed in the past to access M/pyt complexes, including the use of (i) the free ligand with or without added base,[25,33] (ii) the Na(pyt) salt in a metathesis reaction with the metal chloride,[30,39] and (iii) the disulfide version 2,2′-dithiobis(pyridine) in an oxidative addition reaction.[24,30,50] We chose the reaction of Na(pyt) with Cl$^-$-containing V reagents as being the most convenient for our purposes.

$$2VOCl_2(THF)_2 + 4Na(pyt) \rightarrow V_2O_2(pyt)_4 + 4NaCl + 4THF \quad (1)$$

Addition of Na(pyt) to $VOCl_2(THF)_2$ gives a dark brown solution from which can be isolated $V_2O_2(pyt)_4$ (**1**) in good yield (eq 1). Crystals isolated from CH_2Cl_2/hexanes and THF/hexanes are brown and green, respectively, but both lose solvent rapidly to give the same pea green powder, and the different crystal colors are therefore a result of different lattice solvent content. IR spectra of crystals and powder are identical except for solvent bands.

In a similar fashion, the reaction of Na(pyt) with $VCl_3(THF)_3$ gives an intense blood-red color from which can be isolated [VNa(pyt)$_4$(THF)$_2$] (**2**) (eq 2). The reaction gives the same

$$VCl_3(THF)_3 + 4Na(pyt) \rightarrow [VNa(pyt)_4(THF)_2] + 3NaCl + THF \quad (2)$$

product in lower yield and purity when only 3 equiv. of Na-

(49) Chisholm, M. H.; Folting, K.; Huffman, J. C.; Kirkpatrick, C. C. *Inorg. Chem.* **1984**, *23*, 1021.

(50) Mura, P.; Olby, B. G.; Robinson, S. D. *Inorg. Chim. Acta* **1985**, *98*, L21.

(pyt) are employed. Dissolution of complex **2** in CH_2Cl_2 gives a red solution that slowly deposits a white powder identified as Na(pyt) by IR. This suggests that in this solvent the *tris*-chelate complex forms (eq 3), but its isolation was not pursued; it is

$$[VNa(pyt)_4(THF)_2] \rightarrow V(pyt)_3 + Na(pyt) \quad (3)$$

likely to be structurally very similar to the anion in the V^{II} complex $(PPh_4)[V(pyt)_3]$ reported by others.[22,32a]

Extending our efforts to V^{II}, we explored the reaction of Na(pyt) with $VCl_2(tmeda)_2$. This gave a deep purple-red solution, and an extremely air- and moisture-sensitive dark purple solid was isolated, which proved to be $V(pyt)_2(tmeda)$ (**3**) after recrystallization from THF/hexanes (eq 4). Addition of a third

$$VCl_2(tmeda)_2 + 2Na(pyt) \rightarrow V(pyt)_2(tmeda) + 2NaCl + tmeda \quad (4)$$

equivalent of Na(pyt) had no effect. Complex **3** is an extremely rare example of a V^{II} thiolate, the only other examples being $(PPh_4)[V(pyt)_3]$ mentioned above and V(L-S_4)(tmeda) (L-S_4 = a tetradentate S-based ligand).[32b]

The O_2 sensitivity of complexes **2** and **3** was further explored in THF solution. For both complexes, addition of stoichiometric amounts of O_2 at room temperature produced a lighter green-brown color; layering of the solutions with hexanes gave green products identified as complex **1** by IR. The transformations are summarized in eqs 5 and 6. Apparently similar reactions

$$2[VNa(pyt)_4(THF)_2] + O_2 \rightarrow V_2O_2(pyt)_4 + 2Na(pyt) + (pyt)_2 + 4THF \quad (5)$$

$$2V(pyt)_2(tmeda) + O_2 \rightarrow V_2O_2(pyt)_4 + 2tmeda \quad (6)$$

in THF occur with elemental sulfur, rapidly with **3** but less so with **2**; the latter reaction had to be refluxed to ensure complete reaction. The solutions turn an orange-red color, and addition of hexanes causes precipitation of orange-red microcrystalline solids whose IR spectra are identical to each other and very similar to that of **1**, except that the band at 972 cm^{-1} assignable to the vanadyl $[VO]^{2+}$ stretch is absent, and a new band is observed at 582 cm^{-1} characteristic of the thiovanadyl $[VS]^{2+}$ unit. The data are consistent with the products being $V_2S_2(pyt)_4$, the thiovanadyl version of **1**, formed in a manner analogous to the reactions in eqs 5 and 6. However, a crystal structure is required for confirmation of the precise metal nuclearity and structure, and we have been unable to-date to obtain suitable single crystals.

Description of Structures. ORTEP plots of complexes **1**–**3** are shown in Figures 1–3. Fractional coordinates and selected structural parameters for **1**–**4** are listed in Tables 2–9. Complex **1** lies on an inversion center and contains two $[VO]^{2+}$ units monoatomically bridged by two S atoms S(3) and S(3′) from two pyt^- groups whose N atoms are terminally ligated in an equatorial coordination site. These two pyt^- groups are thus bound in mode **IV**, but the S atoms bridge very asymmetrically, and this is an extremely rare variation of mode **IV** binding.[51] Atom S(3), for example, occupies an equatorial site at V(1′) but an axial site at V(1), and the two resultant bond lengths (V(1′)–S(3) = 2.457(4) Å, V(1)–S(3) = 2.798(3) Å) are significantly different, the lengthening of the latter being assignable to the strong *trans* influence of the multiply-bonded $[VO]^{2+}$ unit. A bidentate, chelating pyt^- (mode **I**) completes a highly distorted octahedral geometry at each metal center. The $[VO]^{2+}$ bond (1.583(6) Å) is typical for this unit, and indicates no noticeable lengthening from the presence of a *trans* S atom. The molecule has crystallographically-imposed C_i symmetry.

Complex **2** (Figure 2) contains a rare example of a seven-coordinate V^{III} center[52–55]; there are three chelating pyt^- groups attached to the V, and a seventh bond to the S atom, S(23), which is part of the fourth pyt^- group. The latter is chelating

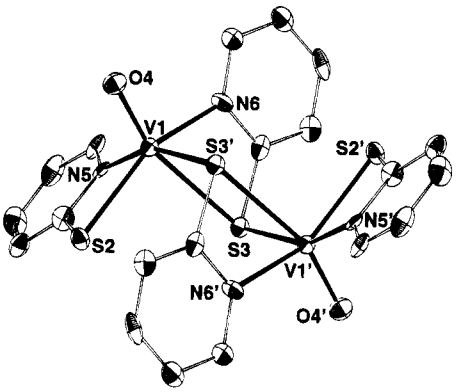

Figure 1. ORTEP representation of $[V_2O_2(pyt)_4]$ (**1**) at the 50% probability level. Primed and unprimed atoms are related by the inversion center.

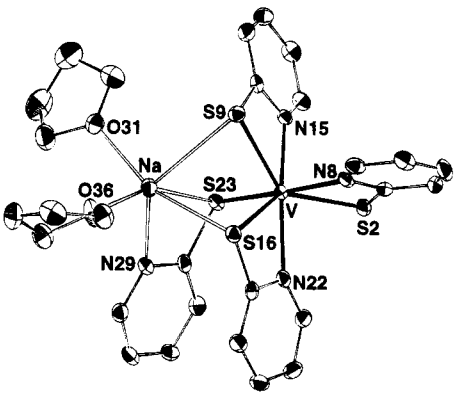

Figure 2. ORTEP representation of $[V(pyt)_4Na(THF)_2]$ (**2**) at the 50% probability level.

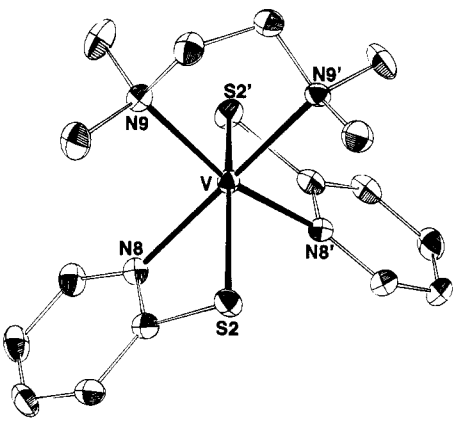

Figure 3. ORTEP representation of $[V(pyt)_2(tmeda)]$ (**3**) at the 50% probability level.

(51) To our knowledge, only one example of this ligation mode has been reported. See: Castano, M. V.; Macias, A.; Castineiras, A.; Gonzalez, A. S.; Martinez, E. M.; Casas, J. S.; Sordo, S.; Hiller, W.; Castellano, E. E. *J. Chem. Soc., Dalton Trans.* **1990**, 1001.

(52) Vuletic, N.; Djordjevic, C. *J. Chem. Soc., Dalton Trans.* **1973**, 1137.
(53) Drew, R. E.; Einstein, F. W. B. *Inorg. Chem.* **1973**, *12*, 829.
(54) Levenson, R. A.; Dominguez, R. J. G.; Willis, M. A.; Young, F. R., III. *Inorg. Chem.* **1974**, *13*, 2761.
(55) Begin, D.; Einstein, F. W. B.; Field, J. *Inorg. Chem.* **1975**, *14*, 1785.

Table 2. Selected Fractional Coordinates ($\times 10^4$) and Equivalent Isotropic Thermal Parameters ($\times 10$)[a] for $[V_2O_2(pyt)_4]\cdot 2THF\cdot {}^1/_3C_6H_{12}$

atom	*x*	*y*	*z*	B_{eq}, Å^2
V(1)	5611(1)	172(1)	6189(2)	13
S(2)	5523(1)	730(1)	7910(2)	16
S(3)	5265(1)	502(1)	3808(2)	14
O(4)	5856(2)	−101(2)	7041(7)	18
N(5)	6216(2)	899(3)	6046(7)	12
N(6)	5722(3)	−13(3)	4017(8)	15
C(7)	6113(3)	1135(3)	7140(9)	16
C(8)	6444(3)	1630(4)	7492(10)	20
C(9)	6881(4)	1870(3)	6722(11)	24
C(10)	6999(3)	1630(4)	5621(11)	23
C(11)	6655(3)	1145(3)	5312(9)	18
C(12)	5552(3)	194(3)	3004(9)	16
C(13)	5609(3)	141(3)	1482(9)	20
C(14)	5830(3)	−131(3)	1028(10)	22
C(15)	5998(3)	−340(3)	2076(10)	21
C(16)	5947(3)	−272(4)	3573(10)	20

[a] $B_{eq} = {}^4/_3\sum\sum B_{ij}a_ia_j$.

Table 3. Selected Fractional Coordinates ($\times 10^4$) and Equivalent Isotropic Thermal Parameters ($\times 10$)[a] for $VNa(pyt)_4(THF)_2$ (**2**)

atom	*x*	*y*	*z*	B_{eq}, Å^2
V(1)	6376(1)	2804.2(4)	7816(1)	11
S(2)	4093(1)	3281(1)	6303(1)	16
C(3)	4173(4)	3691(2)	8159(5)	16
C(4)	3190(4)	4159(3)	8628(5)	21
C(5)	3436(5)	4439(3)	10152(6)	25
C(6)	4646(5)	4266(3)	11197(5)	22
C(7)	5583(4)	3803(3)	10676(5)	19
N(8)	5348(3)	3522(2)	9191(4)	14
S(9)	7240(1)	1884(1)	9830(1)	15
C(10)	5894(4)	1275(2)	8528(4)	15
C(11)	5511(4)	475(3)	8555(5)	19
C(12)	4454(4)	72(3)	7373(5)	20
C(13)	3766(4)	478(3)	6189(5)	20
C(14)	4164(4)	1265(3)	6236(5)	18
N(15)	5205(3)	1666(2)	7390(4)	14
S(16)	8651(1)	3465(1)	9533(1)	15
C(17)	8320(4)	4019(2)	8067(4)	15
C(18)	9177(4)	4597(3)	7879(5)	19
C(19)	8688(5)	5002(3)	6678(5)	22
C(20)	7381(5)	4828(3)	5671(5)	22
C(21)	6605(4)	4238(3)	5889(5)	18
N(22)	7061(3)	3840(2)	7074(4)	14
S(23)	7104(1)	1884(1)	5823(1)	14
C(24)	8375(4)	2371(2)	5382(4)	14
C(25)	8062(4)	2723(3)	4094(5)	18
C(26)	9092(4)	3068(3)	3760(5)	18
C(27)	10409(4)	3048(3)	4715(5)	19
C(28)	10639(4)	2694(3)	5970(5)	18
N(29)	9656(3)	2348(2)	6327(3)	14
Na(30)	9535(2)	1849(1)	8507(2)	17
O(31)	9888(3)	460(2)	8302(3)	22
C(32)	8816(5)	−130(3)	8045(5)	29
C(33)	9266(6)	−948(3)	7417(6)	39
C(34)	10183(6)	−711(3)	6614(6)	42
C(35)	10872(5)	73(3)	7648(6)	31
O(36)	11759(3)	2167(2)	10077(3)	26
C(37)	12991(5)	2003(3)	9721(5)	27
C(38)	14002(5)	1865(3)	11177(6)	31
C(39)	13583(5)	2466(3)	12384(5)	33
C(40)	12171(5)	2700(3)	11549(5)	27

[a] $B_{eq} = {}^4/_3\sum\sum B_{ij}a_ia_j$.

to the Na^+ ion, which is also attached to two S atoms of the pyt^- chelates on the V. Two terminal THF groups complete six-coordination for the Na ion. The initial temptation to describe **2** as an intimate ion-pair between $[Na(THF)_2]^+$ and $[V(pyt)_4]^-$ is resisted; the mode of binding of the pyt^- ligand containing S(23) and N(29) suggests the best description of **2** is as a molecular, triply-bridged, heterobimetallic complex. As for complex **1**, the pyt^- groups in **2** comprise binding modes **I** and **IV**, the latter again in the highly asymmetric form.

Table 4. Selected Fractional Coordinates ($\times 10^4$)[a] and Equivalent Isotropic Thermal Parameters ($\times 10$)[b] for $[V(pyt)_2(tmeda)]$ (**3**)

atom	*x*	*y*	*z*	B_{eq}, Å^2
V(1)	8345.5(4)	5000*	0*	12
S(2)	7977.0(5)	5785.3(4)	2846(1)	17
C(3)	7342(2)	6240(2)	1129(4)	15
C(4)	6837(2)	6908(2)	1324(4)	18
C(5)	6405(2)	7216(2)	−185(5)	22
C(6)	6465(2)	6854(2)	−1869(5)	21
C(7)	6966(2)	6196(2)	−1995(4)	18
N(8)	7392(1)	5890(1)	−533(3)	14
N(9)	9534(2)	5704(1)	−1071(3)	15
C(10)	10369(2)	5417(2)	−97(5)	21
C(11)	9646(3)	5594(2)	−3076(5)	25
C(12)	9466(3)	6517(2)	−718(6)	26

[a] Parameters marked by an asterisk were fixed by symmetry. [b] $B_{eq} = {}^4/_3\sum\sum B_{ij}a_ia_j$.

Table 5. Fractional Coordinates ($\times 10^4$) and Equivalent Isotropic Thermal Parameters ($\times 10$)[a] for pytH (**4**)

atom	*x*	*y*	*z*	B_{eq}, Å^2
C(1)	6631(4)	2652(4)	6139(1)	16
C(2)	7356(4)	4423(4)	6745(2)	18
C(3)	5899(4)	6015(4)	6858(2)	21
C(4)	3621(4)	5936(4)	6387(2)	21
C(5)	2919(4)	4222(4)	5817(2)	18
N(6)	4395(3)	2656(3)	5706(1)	16
S(7)	8346(1)	640(1)	5923.4(4)	19

[a] $B_{eq} = {}^4/_3\sum\sum B_{ij}a_ib_j$.

Table 6. Selected Interatomic Distances (Å) and Angles (deg) for $[V_2O_2(pyt)_4]\cdot 2THF\cdot {}^1/_3C_6H_{12}$

V(1)···V(1′)	3.989(2)	V(1)−N(5)	2.088(7)
V(1)−S(2)	2.427(3)	V(1)−N(6)	2.106(7)
V(1)−S(3)	2.457(4)	S(2)−C(7)	1.756(8)
V(1)−S(3′)	2.798(3)	S(3)−C(12)	1.746(9)
V(1)−O(4)	1.583(6)		
S(2)−V(1)−S(3)	91.65(10)	S(3)−V(1)−N(5)	158.11(19)
S(2)−V(1)−S(3′)	97.76(9)	S(3)−V(1)−N(6)	91.74(21)
S(2)−V(1)−O(4)	108.92(24)	S(3′)−V(1)−N(6)	62.35(21)
S(2)−V(1)−N(5)	68.51(19)	O(4)−V(1)−N(5)	101.13(28)
S(2)−V(1)−N(6)	150.68(21)	O(4)−V(1)−N(6)	96.7(3)
S(3)−V(1)−S(3′)	81.35(9)	N(5)−V(1)−N(6)	93.15(27)
S(3′)−V(1)−O(4)	158.99(24)	V(1)−S(2)−C(7)	79.2(3)
S(3)−V(1)−O(4)	99.47(22)	V(1)−S(3)−V(1′)	98.65(9)
S(3′)−V(1)−N(5)	82.07(18)		

Complex **3** (Figure 3) is a six-coordinate, distorted octahedral mononuclear V^{II} species with two chelating pyt^- groups (mode **I**) and a chelating tmeda group. The molecule has crystallographically-imposed C_2 symmetry; the S(2)−V−S(2′) angle is only 156.05(4)° and the N(8)−V−N(9′) angle is only 164.27(8)°, emphasizing the large distortion of the molecule away from octahedral geometry. The bonds to pyridine-type N atoms (V−N(8) = 2.1244(23) Å) are noticeably shorter than the bonds to tmeda N atoms (V−N(9) = 2.2524(23) Å).

The low-temperature crystal structure of the free ligand in its protonated form was obtained for comparison with the pyt^- groups in **1**−**3**. The pytH molecule exists as a tautomeric equilibrium between the thiol (**A**) and thione (**B**) forms shown.

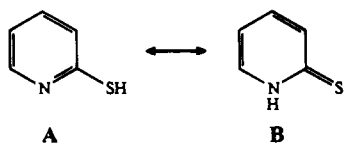

A **B**

Room-temperature diffraction experiments[56] have previously

Table 7. Selected Interatomic Distances (Å) and Angles (deg) for $[VNa(pyt)_4(THF)_2]$ (**2**)

V(1)−S(2)	2.526(1)	V(1)−N(22)	2.187(3)
V(1)−S(9)	2.567(1)	S(2)−C(3)	1.737(4)
V(1)−S(16)	2.543(1)	S(9)−C(10)	1.734(4)
V(1)−S(23)	2.495(1)	S(16)−C(17)	1.735(4)
V(1)−N(8)	2.121(3)	S(23)−C(24)	1.774(4)
V(1)−N(15)	2.178(3)	V(1)· ·Na(30)	3.516(1)
S(2)−V(1)−N(8)	66.58(9)	S(9)−V(1)−N(22)	140.11(14)
S(2)−V(1)−S(9)	136.09(9)	S(16)−V(1)−S(23)	100.06(9)
S(2)−V(1)−N(15)	81.46(14)	N(22)−V(1)−S(23)	86.76(9)
S(2)−V(1)−S(16)	137.24(9)	S(9)−Na(30)−S(16)	63.93(9)
S(2)−V(1)−N(22)	81.11(14)	S(9)−Na(30)−S(23)	77.42(9)
S(2)−V(1)−S(23)	102.76(9)	S(9)−Na(30)−N(29)	130.68(14)
N(8)−V(1)−S(9)	89.45(14)	S(9)−Na(30)−O(31)	96.80(14)
N(8)−V(1)−N(15)	96.05(12)	S(9)−Na(30)−O(36)	120.99(14)
N(8)−V(1)−S(16)	91.58(9)	S(16)−Na(30)−S(23)	82.81(9)
N(8)−V(1)−N(22)	96.32(12)	S(16)−Na(30)−N(29)	87.84(14)
N(8)−V(1)−S(23)	168.16(9)	S(16)−Na(30)−O(31)	159.30(14)
S(9)−V(1)−N(15)	64.39(14)	S(16)−Na(30)−O(36)	91.82(14)
S(9)−V(1)−S(16)	75.87(9)	S(9)−V(1)−S(23)	95.55(9)
N(15)−V(1)−S(16)	139.35(9)	S(23)−Na(30)−N(29)	58.63(14)
N(15)−V(1)−N(22)	152.53(12)	S(23)−Na(30)−O(31)	101.04(14)
N(15)−V(1)−S(23)	76.59(9)	S(23)−Na(30)−O(36)	156.09(14)
S(16)−V(1)−N(22)	64.57(9)	V(1)−S(9)−Na(30)	77.15(9)
N(29)−Na(30)−O(31)	111.65(14)	V(1)−S(16)−Na(30)	80.44(9)
N(29)−Na(30)−O(36)	98.03(14)	V(1)−S(23)−Na(30)	79.96(9)
O(31)−Na(30)−O(36)	92.20(14)		

Table 8. Selected Interatomic Distances (Å) and Angles (deg) for $[V(pyt)_2(tmeda)]$ (**3**)

V(1)−S(2)	2.546(1)	V(1)−N(9)	2.252(2)
V(1)−N(8)	2.124(2)	S(2)−C(3)	1.741(3)
S(2)−V(1)−S(2′)	156.05(4)	N(8)−V(1)−N(8′)	99.89(13)
S(2)−V(1)−N(8′)	97.24(6)	N(8)−V(1)−N(9)	90.65(9)
S(2)−V(1)−N(8)	66.85(6)	N(8)−V(1)−N(9′)	164.27(8)
S(2)−V(1)−N(9)	97.63(6)	N(9)−V(1)−N(9′)	81.64(12)
S(2)−V(1)−N(9′)	100.45(6)	V(1)−S(2)−C(3)	77.43(10)

Table 9. Interatomic Distances (Å) and Angles (deg) for pytH (**4**)[a]

S(7)−C(1)	1.700(2)	C(2)−C(3)	1.363(3)
N(6)−C(1)	1.364(3)	C(3)−C(4)	1.401(3)
N(6)−C(5)	1.357(3)	C(4)−C(5)	1.359(3)
C(1)−C(2)	1.416(3)		
C(1)−N(6)−C(5)	124.32(20)	C(2)−C(3)−C(4)	120.92(23)
S(7)−C(1)−(6)	120.35(16)	C(3)−C(4)−C(5)	117.79(23)
S(7)−C(1)−C(2)	124.55(17)	N(6)−C(5)−C(4)	120.58(22)
N(6)−C(1)−C(2)	115.10(20)		
C(1)−C(2)−C(3)	121.29(22)		

[a] Numbering scheme: S(7)−C(1)−C(2)−C(3)−C(4)−C(5)−N(6)−.

indicated that the H atom is located on the N atom and that the thione tautomer is a major contributor to the tautomeric equilibrium. This conclusion is confirmed by our own low-temperature (−157 °C) study, which also shows insignificant changes to the structural parameters (i.e., to the tautomeric composition) as a function of temperature. The salient features of the structure of pytH (**4**) are as follows: (i) the angle at the N atom (124.32(20)°) is consistent with the protonated form; for pyridine rings, protonated and nonprotonated N atoms possess angles greater or less than 120°, respectively;[57] (ii) owing to the low-temperature data set, the observation of the H atom on the N is reliable, all the H atoms being located in a difference Fourier map and refined; (iii) the six-membered ring shows the variation in C−C bond lengths expected for thione form B rather than the equivalence expected for A, which is aromatic; and (iv) the C−S bond length (1.700(2) Å) is

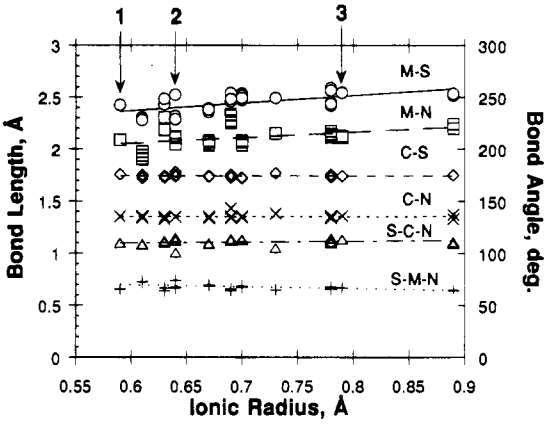

Figure 4. Relationship of M−S, M−N, C−S, and C−N bond lengths and S−C−N and S−M−N bond angles to six-coordinate metal ionic radii for pyt^- ligands in binding mode I from forty-two transition metal/pyt single-crystal X-ray structures. Complexes **1**, **2**, and **3** are indicated by arrows.

significantly shorter than the C−S single bond value typical of the unbound PhS^- group (1.770(5) Å in $(PPh_4)(PhS)$).[58a] The neutral pytH group is often seen as a ligand to soft metals where it functions as an S-bound monodentate ligand.[59] On deprotonation to pyt^- and incorporation into a metal complex, the thiolate form **A** becomes more significant, and the ligand may be approximately and quite adequately described as being deprotonated form **A**, i.e., a thiolate. Restricting further discussion to the present complexes **1**−**3**, the predominantly thiolate (**A**) character of pyt^- is supported by (i) the C−S bonds (1.734(4)−1.774(4) Å), which approach those in $V^{III,IV}$/SPh complexes (1.77−1.80 Å),[58b,c] and (ii) the smaller range of C−C and C−N bond distances within the six-membered rings, which now look more typical of aromatic rings. This shift of the tautomeric equilibrium toward form **A** is as expected for attachment of strongly Lewis acidic M centers, because total electron donation to the latter is facilitated by form **A**, which provides greater electron density at the better σ- and π-donating S atom.

In Figure 4 are compared M−S, M−N, C−S and C−N bond lengths, and S−M−N and S−C−N angles for 42 terminal, chelating (type **I**) pyt^- ligands in various M/pyt^- complexes (including **1**−**3**) as a function of metal ionic radii for six-coordination.[60] The M−S and M−N bond lengths show the expected slight increase with M radius, but it is interesting that the C−S and C−N values are essentially invariant, indicating little if any influence of the M identity on the tautomeric nature (equilibrium) of the ligand. The S−M−N angles become slightly smaller as the ionic radii increase, but this is just strain within the four-membered chelate ring as the M−N/M−S bonds shorten. The average values for the bonds (Å) and angles (deg) are as follows: M−S, 2.445 ± 0.086; M−N, 2.116 ± 0.101; C−S, 1.741 ± 0.015; C−N, 1.351 ± 0.018; S−M−N, 67.62 ± 2.46, and S−C−N, 111.11 ± 3.18. The V−S bond lengths for **2** are a bit longer than expected but this is due to the metal being seven-coordinate, ionic radii for six-coordination having been employed.

(56) Ohms, U.; Guth, H.; Kutoglu, A.; Scheringer, C. *Acta Crystallogr.* **1982**, *B38*, 831.
(57) Kvick, A.; Booles, S. S. *Acta Crystallogr.* **1972**, *B28*, 3405.
(58) (a) Huffman, J. C.; Christou, G. Unpublished results. (b) Nicholson, J. R.; Huffman, J. C.; Ho, D. M.; Christou, G. *Inorg. Chem.* **1987**, *26*, 3030. (c) Dean, N. S.; Bartley, S. L.; Streib, W. E.; Lobkovsky, E. B.; Christou, G. *Inorg. Chem.*, in press.
(59) For recent references, see: (a) Guochen, J.; Puddephatt, R. E.; Vittal, J. J. *Polyhedron* **1992**, *11*, 2009. (b) Hadjikalou, S. K.; Aslanidis, P.; Karagiannidis, P.; Aubry, A.; Skoulika, S. *Inorg. Chim. Acta* **1992**, *193*, 129. (c) Povey, D. C.; Smith, G. W.; Lobana, T. S.; Bhatia, P. K. *J. Cryst. Spectrosc.* **1991**, *21*, 9.
(60) Shannon, R. D.; Prewitt, C. T. *Acta Crystallogr.* **1970**, *B26*, 1076.

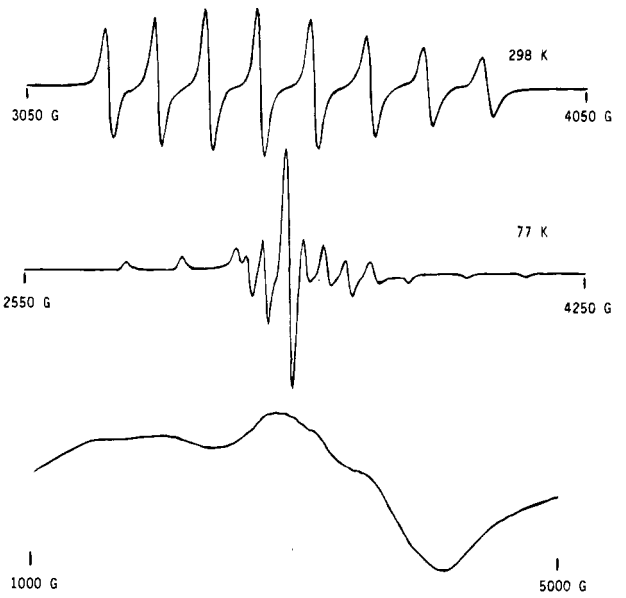

Figure 5. EPR spectra of (A) complex **1** in THF at 298 K, (B) complex **1** in THF at 77 K, and (C) complex **3** in toluene at 115 K.

EPR Spectroscopy. Figure 5a shows the room-temperature X-band EPR spectum of complex **1** in THF solution. The spectrum is a typical eight-line isotropic signal characteristic of mononuclear VO^{2+} species (^{51}V, $I = {}^7/_2$, ~100%), suggesting the dinuclear structure in the solid state is not retained in solution or the metal centers are negligibly interacting. The isotropic parameters, g_{iso} and A_{iso}, calculated using the second-order Zeeman correction, are 1.972 and 97 G, respectively. These values are in the range typical for VO^{2+} square-pyramidal complexes. More detailed relationships between the isotropic parameters of square-pyramidal VO^{2+} complexes and the atoms in the first coordination sphere (N, S, and/or O) have been suggested.[61,62] Compilations of isotropic parameters for VO^{2+} complexes with O_4, S_4, S_2O_2, N_2O_2, and N_4 show, in most cases, an approximately linear relationship between the g_{iso} and A_{iso} values. For an N_2S_2 first-coordination sphere, the g_{iso} and A_{iso} values are predicted from this relationship to be approximately 1.979 and 92 G, respectively, similar but nevertheless different from those for **1**. One of the few examples of a VO^{2+} complex with an N_2S_2 first-coordination sphere, $VO(SCH_2CH(NH_2)CO_2CH_3)_2$,[63,64] has isotropic parameters that also do not agree with those predicted by the above relationship. $[VO]^{2+}$ complexes with minor distortions from square-pyramidal to trigonal-bipyramidal geometry also show deviation from this linear relationship.[65] It is unclear whether this behavior is due to the particular ligands employed or S_2N_2 coordination in general; that it is likely the latter is suggested by 34 GHz EPR studies of 12 VOS_2N_2 complexes (unspecified structures) that indicate that there is no relationship between the g_{iso} and A_{iso} values.[66]

The relatively small bite distance and angle of the pyt^- ligand should have some noticeable effect on the M/pyt bonds compared with metal complexes containing bidentate ligands with larger bites. The degree of M−L covalency in the S_2N_2 complexes can be estimated from the EPR parameters. The Fermi contact term K (the higher the value of K, the less covalent character in the M−L bonds) can be related to the g_{iso} and A_{iso} values and the dipolar term P through eq 7.[67] Using the P value

$$K = [A_{iso} + (2.002 - g_{iso})P]/P \quad (7)$$

of +117 G for VO(8-mercaptoquinoline)$_2$,[68] the K values are 0.86 for **1** and 0.69 for $VO(SCH_2CH(NH_2)CO_2CH_3)_2$, suggesting a significantly higher degree of covalency in the latter.

Figure 5b shows the X-band EPR spectrum at 77 K of a frozen THF solution of **1**. The spectrum is a typical VO^{2+} anisotropic spectrum, exhibiting only partial resolution of the expected 16 lines of an axial system. The spectral parameters are: $g_{\|} = 1.983$, $g_{\perp} = 1.966$, $A_{\|} = 181$ G, and $A_{\perp} = 54$ G. These values are typical for VO^{2+} complexes with N, S, and/or O in the first coordination sphere. In comparison with other N_2S_2 complexes, they are very close to those of VO(8-mercaptoquinoline)$_2$,[68] but show a much lower $g_{\|}$ and much higher $A_{\|}$ than $VO(SCH_2CHNH_2COOCH_3)_2$.[63,64]

The room-temperature X-band EPR spectrum of complex **3** in toluene solution shows a very broad signal centered in the $g \approx 2$ region. In frozen toluene solution at 115 K (Figure 5c), additional broad and ill-defined features become apparent at higher g values. There is some faint indication of hyperfine structure in the upfield signals. The signal is clearly not that of a $S = {}^1/_2$ spin system and in that respect is consistent with a $S = {}^3/_2$ system in rhombic symmetry, as expected for **3**, but little other useful information can be extracted.

Mass Spectrometry. Complexes **1** and **2** have been studied by electron ionization mass spectrometry (EIMS) to determine gas-phase fragmentation pathways and to probe possible C−S bond cleavage reactions. Figure 6 shows the principal fragments for **1** (M = VO), and **2** (M = V). Table 10 lists the m/z and relative intensities for structures ***A***−***H*** in Figure 6, normalized to the parent ion of the complex. Both complexes have very similar fragmentation patterns; smaller ions are formed from the loss of S, pyridine, or pyt^- during the fragmentation process. For **2**, ML_3^+ is the highest intensity ion, which is not the expected ion for the formula $VNa(pyt)_4(THF)_2$. This suggests that Na(pyt) and THF are readily lost from **2**, as also suggested by its behavior in CH_2Cl_2 described earlier. For **1**, ML_2^+ is the highest intensity ion, which also is not expected from the dinuclear structure of **1** in the solid state. Dissociation into mononuclear units is obviously facile under these conditions.

The next highest intensity ion for **2** is the ML_2^+ fragment, which is the highest intensity ion for **1**. Other fragments of both complexes are similar, differing only by M = V or VO.

Table 10. Principal Ions and their Intensities in EIMS Examination of $[V_2O_2(pyt)_4]$ (**1**) and $[VNa(pyt)_4(THF)_2]$ (**2**)

species	**1** (M = VO)[a]	**2** (M = V)[a]
A	na	380 (100)
B	287 (100)	271 (80)
C	254 (4)	238, 239 (35)
D	208, 209 (10)	192, 193 (22)
E	223 (38)	207 (5)
F	177 (47)	161 (14)
G	145 (13)	129 (5)
H	99 (2)	83 (9)

[a] *M/z* (relative intensity). na = not applicable.

(61) Yen, T. F.; Boucher, L. J.; Dickie, J. P.; Tynan, E. C.; Vaughan, G. B. *J. Inst. Pet.* **1969**, *55*, 87.
(62) Dickson, F. E.; Kunesh, C. J.; McGinnis, E. L.; Petrakis, L. *Anal. Chem.* **1969**, *44*, 978.
(63) Sakurai, H.; Taira, Z.-E.; Sakai, N. *Inorg. Chim. Acta* **1988**, *151*, 85.
(64) Sakurai, H.; Hamada, Y.; Shimomura, S.; Yamashita, S. *Inorg. Chim. Acta* **1980**, *46*, L119.
(65) Shiro, M.; Fernando, Q. *Anal. Chem.* **1971**, *43*, 1222.
(66) Malhotra, V. M.; Buckmaster, H. A. *Fuel* **1985**, *64*, 335.
(67) Boucher, L. J.; Tynan, E. C.; Yen, T. F. In *Electron Spin Resonance of Metal Complexes, Proceedings*; Yen, T. F., Eds.; Plenum Press: New York, 1969.
(68) Jezierski, A.; Jezowska-Trzebiatowska, B. *Bull. Pol. Acad. Sci., Chem.* **1985**, *33*, 85.

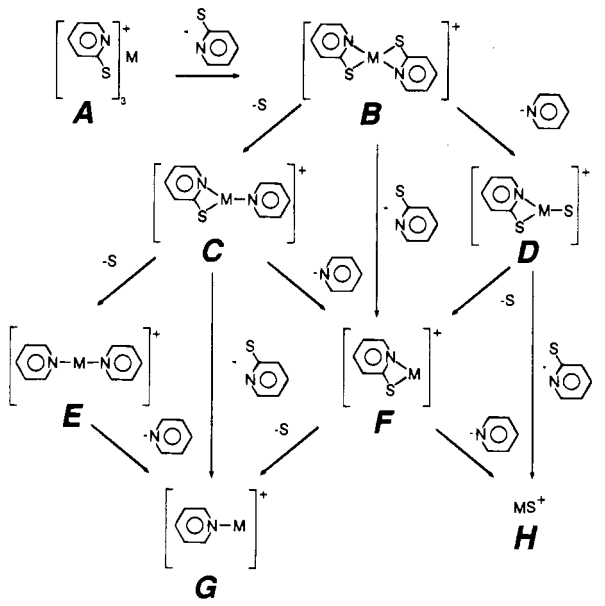

Figure 6. EIMS fragmentation patterns for complexes **1** and **2**. Fragment *m/z* values and relative intensities are listed in Table 10.

The intensities of these fragments, however, differ markedly depending on whether they are from **1** or **2**. For example, **1** exhibits a prominent ion with only one ligand (structure ***F***). The analogous fragment for **2** is not nearly as intense. Fragments ***C*** and ***D*** for **2** are reasonably intense, but fragments ***E*** and ***F*** are not. For **1**, the relative intensities of these fragments are reversed; fragments ***C*** and ***D*** are not intense, while fragments ***E*** and ***F*** are. Thus, complexes **1** and **2** show noticeable differences in the fragmentation behaviors that can reasonably be attributed to the main difference between the complexes, namely, the presence of a multiply-bonded [VO] unit. Its presence appears to facilitate/stabilize the smaller fragments ***E*** and ***F*** whereas these are too unstable and short-lived for **2**. This suggests that the oxidation state of the metal center and strong ancillary ligation can be important in controlling the fragmentation pathways of **1** and **2**; similar effects have been seen in the fragmentation pathways of other vanadium complexes studied by EIMS.[69,70]

(69) MacDonald. C. G.; Shannon, J. S. *Aust. J. Chem.* **1986**, *19*, 1545.

The above study was undertaken with the belief that the results might be of utility as a model system for some of the high-energy reactions occurring during hydrodemetalation (HDM)−hydrodesulfurization (HDS) petroleum processes. Clearly, under normal ionization conditions, both compounds **1** and **2** show one or more fragmentation pathways involving C−S bond cleavage, as previously detected in $[V(SBu^t)_4]$ where the C−S bonds are more easily cleaved.[17] For example, $[VO(C_5H_4NS)_2]^+$ (***B***) gives fragment ions assigned to $[VO(C_5H_4NS)(C_5H_4N)]^+$ (***C***), $[VO(C_5H_4N)_2]^+$ (***E***), and $[VO(C_5H_4NS)S]^+$ (***D***) that appear to form through a one- or two-step process involving C−S bond cleavage. The ion $[V(C_5H_4NS)_3]^+$ responds similarly under the same conditions, producing $[V(C_5H_4NS)_2]^+$ (***B***) which gives $[V(C_5H_4NS)(C_5H_4N)]^+$ (***C***), $[V(C_5H_4N)_2]^+$ (***E***), and $[V(C_5H_4NS)S]^+$ (***D***) *via* the same C−S bond cleavage processes. Extrapolating the gas-phase fragmentations observed in this study to the similarly high-energy conditions of HDS/HDM provides a credible pathway for the conversion of (i) molecular V/organosulfur impurities in crude oils into V/S polymer deposits (V_2S_3/V_3S_4) and/or (ii) the binding of free organosulfur molecules onto the surface V atoms of a V_2S_3/V_3S_4 solid followed by V-catalyzed C−S bond cleavage providing new S atoms for the growing V_2S_3/V_3S_4 phase.

Acknowledgment. The work at Lawrence Livermore National Laboratory was performed under the auspices of the U.S. Department of Energy under Contract No. W-7405-ENG-48. Work at Indiana University was supported by the Office of Basic Energy Sciences, Division of Chemical Sciences, U.S. Department of Energy, Grant DE-FG02-87ER13702. We thank Norman S. Dean for assistance with EPR spectroscopy.

Supporting Information Available: Text detailing the structure refinement, figures showing the basic structure and unit cell, and complete listings of atomic coordinates, isotropic and anisotropic thermal parameters, bond distances and angles (40 pages). Ordering information is given on any current masthead page. Listings of observed and calculated structure factors for **1**−**4** are available from the author on request. Complete MSC structure reports (Nos. 91014 for **1**, 91150 for **2**, 92011 for **3**, and 89020 for **4**) are available on request from the Indiana University Chemistry Library.

IC9503702

(70) Charalambous, J. J. In *Mass Spectrometry of Metal Compounds*; Charalambous, J., Ed.; Butterworths: London, 1975; pp 45−60.